Macromolecules
ARTICLE

Macromolecules **2009**, *42*, 6215–6224 **6215**
DOI: 10.1021/ma900885b

Morphology Development in Thermosetting Mixtures through the Variation on Chemical Functionalization Degree of Poly(styrene-*b*-butadiene) Diblock Copolymer Modifiers. Thermomechanical Properties

Connie Ocando,[†] Agnieszka Tercjak,[†] M. Dolores Martín,[†] José A. Ramos,[†] Mónica Campo,[‡] and Iñaki Mondragon*,[†]

[†]*"Materials + Technologies" Group, Escuela Politécnica, Dpto. Ingeniería Química y M. Ambiente, Universidad del País Vasco/Euskal Herriko Unibertsitatea, Pza. Europa 1, 20018 Donostia-San Sebastián, Spain, and* [‡]*Dpto. Ciencia e Ingeniería de Materiales, ESCET, Universidad Rey Juan Carlos, C/Tulipán s/n, 28933 Madrid, Spain*

Received April 22, 2009; Revised Manuscript Received July 20, 2009

ABSTRACT: Recently we reported the critical content threshold of epoxidized polybutadiene (PBep) units to induce total miscibility between poly(styrene-*b*-butadiene) (SB) block copolymers (BC) and uncured epoxy resin.[20] In this work we investigate the different mechanisms involved through morphology development, depending on the content of epoxidized polybutadiene (PBep) in the initial mixture. PBep contents higher than, close below, or far below the critical threshold lead to long-range order nanostructures through reaction-induced microphase separation (RIMS) of PS block, a combination of both self-assembly and RIMS leading to vesicles or long wormlike micelles with a bilayered structure, or macroscopic phase separation, respectively. Nanoindentation was employed to identify the microphase-separated domains. Epoxy matrix can be significantly toughened for high BC contents in both *prior to* or *through* curing microphase-separated mixtures. Phase-separated domain size but also extent of interactions between them and their shape seem to be the factors contributing to toughness enhancement.

1. Introduction

The modification of epoxy resins with block copolymers has been in the past years a great research source due to the capability of block copolymers (BC) to act as templates for the synthesis of long-range order nanostructured thermosetting matrices. For this purpose, two mechanisms of morphology formation during curing have been proposed. The first way reported for creating nanostructures in epoxy networks arises via self-assembly where the epoxy resin can act as selective solvent for one of the BC blocks.[1−6] In this mechanism the block immiscible with the epoxy precursor segregates before curing to produce an initial microphase-separated mixture. Then, the microphase-separated morphology can be fixed in the matrix through curing. On the other hand, the second mechanism is through reaction-induced microphase separation.[7−14] In this case, both blocks in the copolymer must be initially miscible with the epoxy resin. Through curing only one block is demixed to generate microphase-separated domains.

In order to promote the compatibilization of one of the blocks with the epoxy resin, block copolymers can be chemically modified. Indeed, poly(styrene-*b*-butadiene) (SB) block copolymers can be randomly epoxidized with hydrogen peroxide in the presence of a catalyst in a biphasic system.[15] This method of functionalization is a feasible approach to promote the compatibilization of PB block with the epoxy resin.[16] Polystyrene (PS) homopolymer was found miscible with the epoxy resin at temperatures higher than 90 °C.[3] Previous work of our group reported the process for obtaining a new family of nanostructured epoxy matrices with long-range order in the bulk due to reaction-induced microphase separation of PS block.[17−20] Additionally, previous studies about the reactivity of epoxidized PB block in these epoxy systems showed that the oxirane groups present in this block are able to react with the thermosetting formulation. However, it was found that the reactivity of epoxidized PB units with the hardener was notably lower than that corresponding to the epoxy groups of DGEBA monomer.[19] The preparation of nanostructured materials by modification with block copolymers can further optimize the fracture toughness properties of brittle epoxy matrix maintaining the transparency of neat materials.[21−30] Different mechanisms like debonding, cavitation, and crack deflection have been proposed to account for the toughening of the epoxy matrix. For example, Sue and co-workers reported the nanoscale cavitation of spherical micelles as toughening mechanisms in block copolymer-modified epoxy systems.[31−33]

The goal of this work was to study the different mechanisms involved in the morphology development in thermosetting epoxy matrices (EP) modified with linear poly(styrene-*b*-butadiene) diblock copolymers epoxidized at several degrees. Varying the compatibilization degree of PB block, the microstructures of the mixtures develop either by an initial microphase separation of one block or by reaction-induced microphase separation. The morphologies changed from macroscopic phase-separated domains to no-large-range order nanostructured domains and to long-range order microphase-separated domains for low epoxidation degree, near to or higher than the critical epoxidation threshold of butadiene blocks, respectively. Fracture toughness of these systems seems to be closely related to their morphology but also to the extent on interactions between phases.

*Corresponding author: e-mail inaki.mondragon@ehu.es, tel +34-943017271, fax +34-943017200.

Published on Web 07/29/2009

2. Experimental Section

2.1. Epoxidation and Characterization of Epoxidized SB Block Copolymers. Anionic polymerization synthesized linear poly(styrene-*b*-butadiene) diblock copolymers, SB50 and SB65, were used. These BC were kindly supplied by Repsol-YPF. The number-average molecular weight for SB65 is 40 000 and polydispersity 1.12. Two SB50 with different number-average molecular weights were used: SB50(1) and SB50(2) with 40 000 and 80 000 g/mol and polydispersities 1.16 and 1.24, respectively. SB50(1) was also used to achieving high epoxidation degree, as it was hard to obtain with SB50(2). The fraction of PB block was 50 wt % (46 wt % 1,2-PB) for both SB50 and 65 wt % (47 wt % 1,2-PB) for SB65. SB block copolymers epoxidized at several degrees, SB-(50 or 65)epI, epI being the epoxidation mol % with respect to PB double bonds, were obtained by epoxidation of polybutadiene block (PBep). The epoxidation reaction was carried out using hydrogen peroxide in the presence of an *in situ* prepared catalyst system in a water/dichloroethane biphasic system. The details of the reaction are described elsewhere.[15,16] The characteristics of these copolymers are listed in Table 1. ^{1}H nuclear magnetic resonance (^{1}H NMR) spectra recorded in deuterated chloroform solution with a Bruker 300 MHz spectrometer at 25 °C were used to determine the epoxidation degree.

2.2. Block Copolymer/Epoxy Mixtures. *Thermoset Precursors*. The epoxy resin used, diglycidyl ether of bisphenol A (DGEBA), DER 332, was gently supplied by Dow Chemical. It has an epoxy equivalent around 175 and an average number of hydroxyl groups per two epoxy groups $n = 0.03$. The hardener used was an aromatic diamine, 4,4′-methylenebis(3-chloro-2,6-diethylaniline) (MCDEA), a gift from Lonza. An amino-hydrogen-to-epoxy stoichiometric ratio equal to 1 was used for all systems, the glass transition temperature (T_g) of epoxy resin before curing being −12 °C, as measured by differential scanning calorimetry.

Blending Protocol. Copolymer/epoxy systems were cured in the following way: first, the copolymer and the DGEBA resin were dissolved in toluene. The resultant solution was heated at 80 °C in an oil bath and then under vacuum up to complete solvent removal. Then MCDEA was added to the initial mixture, the temperature raised up to 140 °C, and mixed for 5 min. The samples were degassed under vacuum and cured in parallelepipedic molds at 140 °C for 24 h and postcured at 165 °C for 2 h. It has to be emphasized that, even for the maximum degree of epoxidation in SBep block copolymers, the epoxy/amine stoichiometric ratio was not significantly modified.

2.3. Characterization. *Morphological Analysis*. The morphology of the mixtures was studied by atomic force microscopy (AFM). Transmission electron microscopy (TEM) was used to analyze the morphology at higher magnifications. AFM images were obtained with a Nanoscope IIIa scanning probe microscope (Multimode, Digital Instruments). Tapping mode (TM) in air was employed using an integrated tip/cantilever (125 μm in length with ca. 300 kHz resonant frequency). Typical scan rates during recording were 0.7−1 line s^{-1} using a scan head with a maximum range of 16 × 16 μm. Samples of cured mixtures were prepared using a ultramicrotome (Leica Ultracut R) equipped with a diamond knife. For TEM studies, thin sections were microtomed at room temperature using an ultramicrotome Leica EMFCS instrument equipped with a diamond knife. In order to reach contrast between PS, PB, and epoxy phases, the samples were stained with a 0.5 wt % aqueous solution of RuO_4 for 4−10 min. RuO_4 preferentially stains PS microdomains for the system examined (appearing black in the micrographs). The staining time of samples was carefully chosen to avoid the possibility of staining all the phases in the investigated systems. A Philips Tecnai 20 transmission electron miscroscope operated at 200 kV with 2.5 Å resolution was used.

Nanoindentation. Nanomechanical characterization of microphase-separated domains in the mixtures was carried out by AFM in tapping mode at room temperature using a Dimension 3100 microscope and Nanoscope IV controller, from Veeco, Digital Instruments. A rectangular stainless steel cantilever with a diamond tip type DNISP, Veeco, was used to perform indentations. The cantilever spring constant was about 217 N/m, resonant frequency 58 kHz, contact sensitivity 225 nm/V, and a rotation angle of 12°. Calibration was performed on sapphire surface, where any deflection of the cantilever is due to the vertical movement of the piezo without penetration. Force indentation (F) values were determined by Hooke's law, $F = k_h d$, where k_h is the spring constant in N/m and d is the deflection of the cantilever. Indentation depth (h) was derived from the difference between the total piezo-scanner displacement and the deflection of the cantilever. Thus, it was possible to represent F vs h. Analysis of force−indentation curves was made following Oliver and Pharr's work,[34] which assigned the slope of the unloading curve at the point of maximum load (P_{max}) with stiffness (S).

The determination of the nanomechanical properties of the sample requires a well-characterized tip (i.e., spring constant and radius of curvature). Since the tip parameters were not well-known, we limited our experiments to relative measurements of the variation of stiffness of the different phases deduced from the slope of the unloading curve.

Differential Scanning Calorimetry (*DSC*). Glass transition temperatures were determined by using a differential scanning calorimeter Mettler Toledo DSC-822, under a nitrogen flow of 20 mL min^{-1}, working with 5−7 mg samples in aluminum pans. Dynamic scans were performed from −60 to 220 °C at heating rates of 20 °C min^{-1}. The values of T_g were determined at the end-set point of the change in heat capacity.

Dynamic Mechanical Analysis (*DMA*). DMA was carried out on cured mixtures with a Perkin-Elmer DMA7 in three-point bending mode in order to obtain storage modulus, E', and loss factor, tan δ. The temperature associated with the α relaxation is defined as T_α. Scans were carried out at a frequency of 1 Hz and a heating rate of 5 °C min^{-1}, using a span of 5 mm. The samples used were parallelepipedic bars (24 × 3 × 1 mm^3). During the scans the samples were subjected to a static force of 110 mN and a dynamic force of 100 mN. Arbitrary units were used for plotting E' results taking as unity reference the neat epoxy matrix.

Flexural Tests. The mechanical behavior of the cured mixtures was determined in a universal testing machine Instron 4206. Three-point flexural tests were performed. The samples were parallelepipedic bars of 26 × 6 × 1.5 mm^3. The crosshead rate was 0.5 mm min^{-1}. Flexural modulus was determined as the slope of the load−displacement curve in the zone of linear elasticity.

Fracture Toughness Tests. The fracture toughness of these mixtures was evaluated in terms of stress-intensity factor (K_{Ic}) and strain energy release rate (G_{Ic}). An approximate estimation of the critical stress intensity factor, K_{Ic}, values was obtained from three-point bending test performed on single edge notched specimens (SENB) and following the procedure proposed by Williams and Cawood.[35] The tests were performed at a crosshead rate of 10 mm min^{-1}. At least five measurements were

Table 1. Characteristics of the Diblock Copolymers Used

block copolymer	epoxidation degree[a]	T_g(PBep)[b] (°C)
SB50	0	
SB50(2)ep15	15	−34
SB50(2)ep22	22	−27
SB50(1)ep35	35	−17
SB65	0	
SB65ep28	28	−21

[a] Defined as mol % of epoxidized polybutadiene units, as determined by ^{1}H NMR analysis. [b] The T_g of PS block (as measured by DSC) appears around 90 °C for SB50(2) and 80 °C for SB50(1) and SB65 block copolymers.

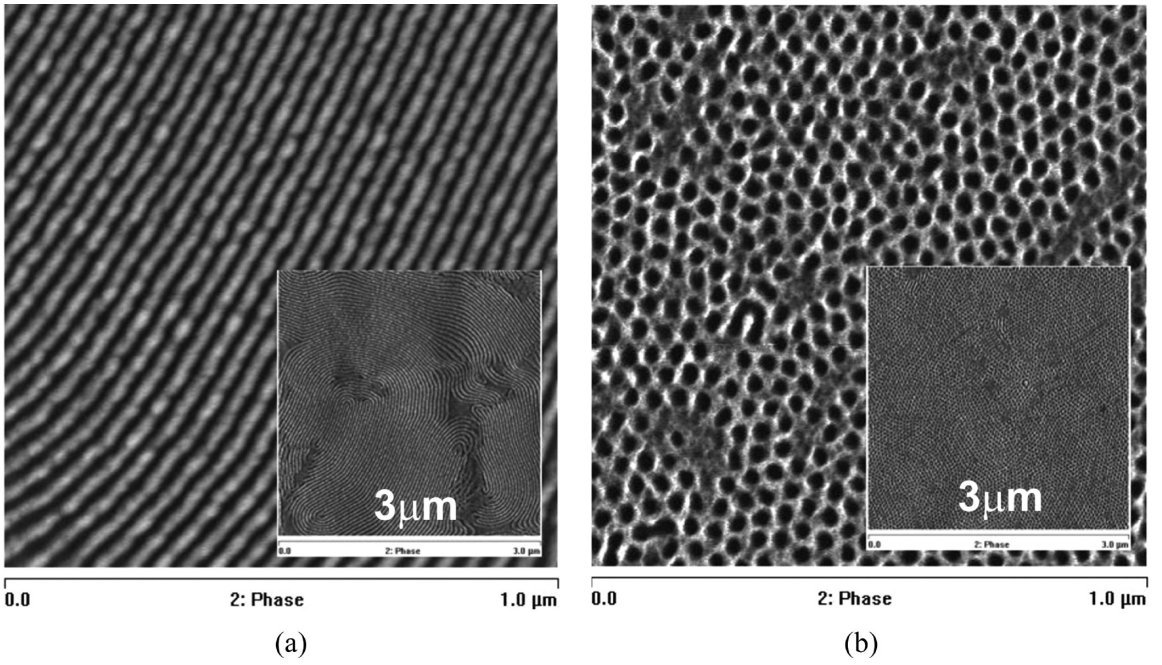

Figure 1. TM-AFM phase images for (a) SB50(1) and (b) SB65, annealed at 110 °C in vacuum for 13 h.

carried out per sample. The samples were parallelepipedic bars of $26 \times 6 \times 1.5$ mm^3, being the notch of around 2.7 mm and the microcracked zone around 0.6 mm. The critical strain energy release rate (G_{Ic}) was calculated from K_{Ic}.

3. Results and Discussion

The morphological behavior of the linear SB diblock copolymers used was first analyzed by microscopy. TM-AFM phase images for the air−surface morphologies of SB thin films prepared by solvent-casting and then annealed at 110 °C in vacuum for 13 h are shown in Figure 1a,b. SB50(1) and SB65 diblock copolymers self-assembled into lamellar and cylindrical nanodomains, respectively. Subsequently, in order to promote compatibilization between the block copolymer modifiers and the epoxy resin, the epoxidation of SB block copolymers was carried out using hydrogen peroxide in the presence of a catalyst prepared *in situ*.[26,27] Table 1 lists the characteristics of the obtained epoxidized block copolymers.

As shown in Figure 2, the cured thermosetting mixture containing 30 wt % of unmodified SB50(2) revealed a block copolymer macrophase separated from the epoxy system as epoxy (EP) and BC phases were clearly discernible at micrometer scale. Though no shown here, SB50(1) also macrophase separated, being these both modified epoxy systems opaque before and after curing due to the lack of interactions of the unepoxidized polybutadiene block and epoxy matrix. SB block copolymers epoxidized at several degrees, 15, 22, and 35 mol %, were added into the epoxy system at different contents, from 10 to 30 wt %, in order to prepare a variety of nanostructured thermosetting systems. First, a visual study about the transparency of the initial mixtures showed that the epoxy systems modified with SB50(2)ep22 were translucent and the epoxy systems modified with SB65ep28 and SB50(1)ep35 were transparent before curing. This observation suggested that the initial mixtures could be miscible or at least microphase separated. On the contrary, in the case of SB50(2)ep15 the initial mixture was opaque. In the following sections, we present a study by AFM and TEM analyses about the mechanisms of microstructure development when the miscibility degree between both components was varied in the mixture. The miscibility of epoxidized

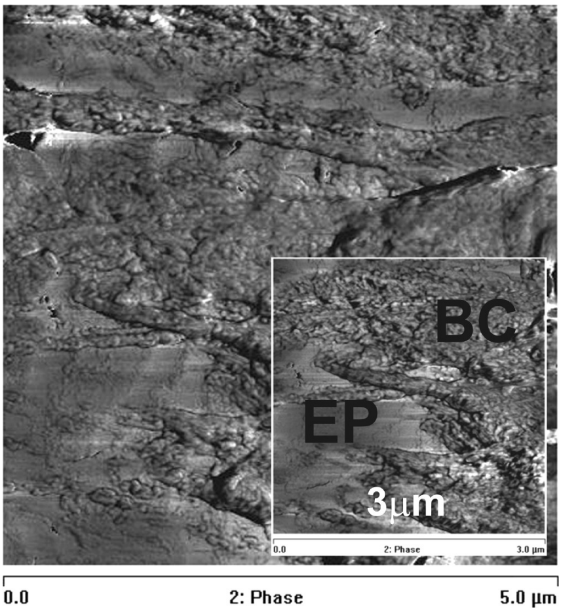

Figure 2. TM-AFM phase image for epoxy mixture containing 30 wt % SB50(2).

block copolymers with the epoxy network was studied by thermal analyses using DSC and DMA. In addition, nano- and macromechanical properties of final mixtures were also analyzed.

Macrophase-Separated Structures in Epoxy Systems Containing SB50(2)ep15 Block Copolymer. SB50(2) block copolymer with 15 mol % of PB block epoxidation was added into the epoxy resin at two different contents, 10 and 30 wt %. Before curing, both mixtures were homogeneous but opaque. AFM and TEM micrographs for these mixtures are shown in Figure 3a,b. As can be seen, these systems presented macrophase separation, suggesting that this epoxidation degree was not enough to develop nanostructured epoxy systems. In a previous work with similar thermosetting mixtures containing 30 wt % of epoxidized SBS triblock copolymer,[20] the minimum threshold established of PBep

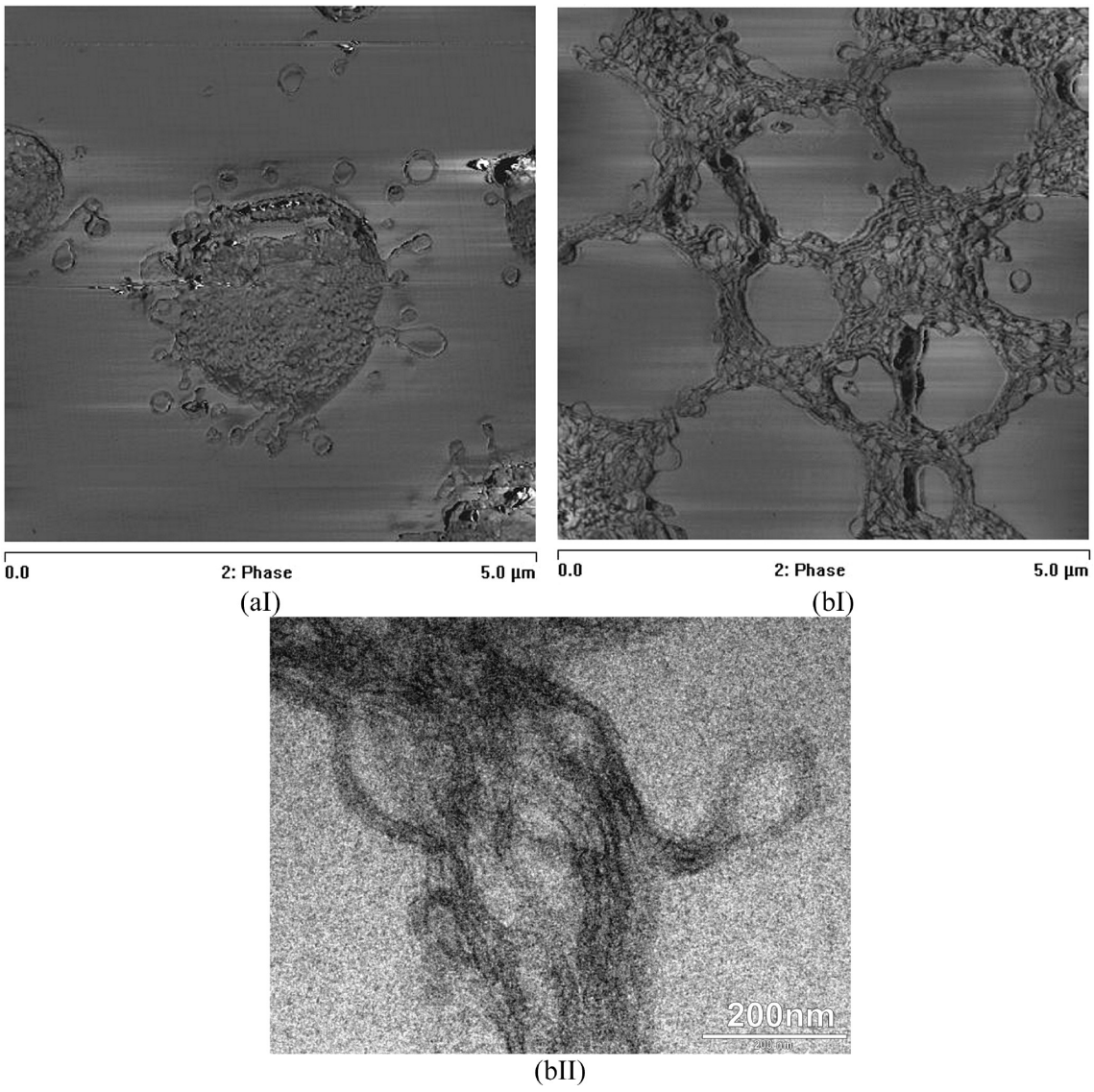

Figure 3. TM-AFM phase (I) and TEM (II) images for epoxy mixtures containing SB50(2)ep15: (a) 10 wt % and (b) 30 wt %. PS block appears dark in AFM images and black in TEM images. RuO_4 preferentially stains PS.

units in the overall mixture to ensure nanostructuring was 4.8 wt %. Consequently, taking into account that for the mixture containing a 30 wt % of SB50(2)ep15 this value is equal to 2.8 wt % of PBep in the overall mixture, one can conclude that in this system macrophase separation should be expected. Dispersed block copolymer domains with size range of 2 μm in a continuous epoxy matrix were observed in 10 wt % SB50(2)ep15 modified system (Figure 3a). Moreover, a phase-inverted morphology was obtained for 30 wt % SB50(2)ep15 modified system, where big domains of epoxy were dispersed in a continuous matrix formed by interconnected rod/wormlike micelles of block copolymer (Figure 3bI,II). Similar results were reported by other authors for an epoxy system modified with a polystyrene (PS) homopolymer,[36] showing dispersed PS domains at low thermoplastic concentrations and a phase-inverted morphology at high thermoplastic concentrations.

The evaluation of glass transition behavior of full reacted mixtures by means of dynamic mechanical analyses is shown in Figure 4. The neat epoxy showed a single T_α around 190 °C. As can be seen, the mixtures containing SB50(2)ep15 revealed a new transition around 90 °C related to the T_α of phase-separated PS block, less distinguished in 15 wt % SB50(2)ep15 mixture due to the lower amount of segregated PS phase. The T_α of epoxy-rich phase in the SB50(2)ep15 mixtures appeared around 180 °C, thereafter showing the rubber plateau in the storage modulus. On the other hand, the 30 wt % SB50(2)ep15 mixture clearly presented a T_α at around 140 °C, which could correspond to high plasticized epoxy-rich phase. Additionally, after the T_α of epoxy rich-phase, the mixture showed a liquidlike behavior, which means that the mixture matrix was the block copolymer. These results support the above shown AFM and TEM analyses.

Microphase-Separated Structures in Epoxy Systems Containing SB50(2)ep22 and SB50(1)ep35 Block Copolymers. The mixtures containing SB50(2)ep22 were translucent after curing, indicating that macrophase separation was absent at this degree of epoxidation. Figure 5a−c shows the AFM (I) and TEM (II) micrographs of thermosetting mixtures containing 10, 20, and 30 wt % SB50(2)ep22 block copolymer. It can be seen that microphase-separated morphologies were developed in all the mixtures. For the 10 wt % SB50(2)ep22 mixture, block copolymer vesicles of several sizes possibly encasing within them epoxy system appeared well dispersed in a continuous epoxy matrix (Figure 5aI). In addition, these

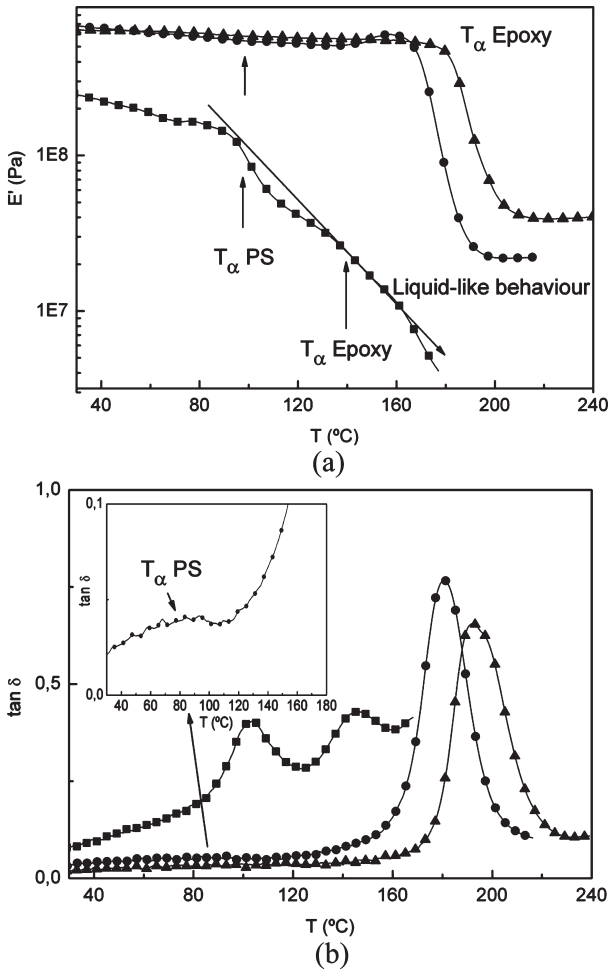

Figure 4. DMA spectra of (a) storage modulus, E', and (b) loss factor, tan δ, obtained at 1 Hz for neat epoxy (▲) and its mixtures containing SB50(2)ep15: 10 wt % (●) and 30 wt % (■).

vesicles presented a layered structure as two phases were discernible in each vesicle domain (Figure 5aII). PS layer appears black in TEM image because the preferential RuO_4 staining. As for this epoxidation degree PS block separated later than epoxidized butadiene block, the outer layers of vesicle shells can be ascribed to PS layers and the inner layer to PBep, being the core related to epoxy system. Additionally, some multivesicular domains can be observed, where many nonconcentric small (daughter) vesicles reside in a much large (mother) one.[37] As can be seen in Figure 5bI,II, increasing the content of block copolymer to 20 wt % in the mixture, the morphology undergoes a transition to interconnected long wormlike micelles. The mixture containing 30 wt % SB50(2)ep22 (Figure 5cI) revealed an entirely long wormlike morphology, also presenting the bilayered structure inside the epoxy matrix where layers of PBep were surrounded by PS layered domains (Figure 5cII). Similar structures have been widely reported in block copolymer in solution (especially in water).[38−42] These morphologies can be explained taking into account that SB50(2)ep22 block copolymer presents an epoxidation degree not enough to make compatible all the PBep block with the epoxy resin before curing, as only a 4 wt % of PBep units does exist in the overall 30 wt % SB50(2)ep22 mixture, being this amount lower than the threshold established to produce nanostructured systems (4.8 wt % of PBep units in mixtures containing 30 wt % of a similar BC).[20] Then, considering the initial miscibility of PS chains and partial miscibility of PBep subchains with the precursors of epoxy resin before curing, it is judged that the formation of the nanostructures in the epoxy network occurs according to this sequence: first, the mechanism of self-assembly of PBep block prior to curing, followed by fixing these nanostructures via phase separation of PS chains through curing reaction.[14]

On the other hand, the dynamic mechanical behavior of full reacted mixtures containing 10−30 wt % SB50(2)ep22, studied by DMA, is shown in Figure 6a,b. As can be seen, all the mixtures presented the T_α of PS block at around 90 °C (more clearly distinguished in 30 wt % SB50(2)ep22 mixture). The T_α of the epoxy matrix appeared at about 180, 175, and 165 °C for 10, 20, and 30 wt % SB50(2)ep22, respectively, thus indicating a plasticization increasing upon block copolymer content. At temperatures higher than T_α of the epoxy-rich phase, all the systems showed a rubberlike behavior (Figure 6a), thus indicating epoxy phase remained as the matrix of these systems. Additionally, DMA and DSC scans of fully reacted mixtures were conducted at low-temperature range (not show here). The thermograms revealed the T_g of PBep block around −30 °C, suggesting that effectively epoxidized polybutadiene block was microphase separated in the mixture.

Furthermore, in order to corroborate that the bilayered vesicles encased the epoxy matrix within them, a nanoindentation analysis using the AFM technique was carried out on both inner and outer regions of a vesicle shell for the 10 wt % SB50(2)ep22 mixture. Figure 7 shows force−indentation curves for these regions. As can be seen, both phases presented a similar stiffness of 190 nN (calculated as explained in experimental part), thus confirming their similar composition based on epoxy matrix.

An AFM image of mixture containing 30 wt % SB50-(1)ep35 is presented in Figure 8. It is worth noting that this mixture exhibited microphase-separated morphology, where hexagonally packed PS cylinders oriented parallelly and perpendicularly to the cutting surface appeared confined with long-range order in the epoxy matrix. This fact suggests that the resulting morphologies originated through reaction-induced microphase separation of PS block starting from a totally miscible mixture before curing. In this case, the epoxidation degree was enough to make compatible the entire PBep block with the epoxy precursor as the total amount of PBep in the mixture was 6.2 wt %, far beyond the minimum threshold established.[20] Moreover, it is important to emphasize that the higher miscibility of SB50-(1)ep35 with the epoxy matrix with respect to SB50(2)ep22 can be also expected due to the differences in molecular weight between these two block copolymers. The microphase separation of PS block was corroborated by DMA experiments (not shown here) as the curves revealed two T_α's, the first at around 80 °C attributed to PS microdomains and the second at 165 °C ascribed to the T_α of epoxy matrix containing PBep chains. On the other hand, by using the Fox equation and the T_α values of epoxy-rich phase in the modified epoxy systems, no big changes in the concentration of epoxidized PB units dissolved in the epoxy-rich phase between the SB50(2)ep22 and SB50(1)ep35-modified epoxy systems were observed, which means the minimum threshold for nanostructuration is found in this range of epoxidation.

Microphase-Separated Structures in Epoxy Thermoset Containing SB65ep28 Block Copolymer. In order to corroborate the strong influence of epoxidation degree of PB block in the mechanism of phase separation, a SB65 block copolymer with higher content of PB block was also added to the epoxy system. The mixtures containing 10 and 30 wt % SB65ep28 were transparent after curing. Figure 9a,b shows

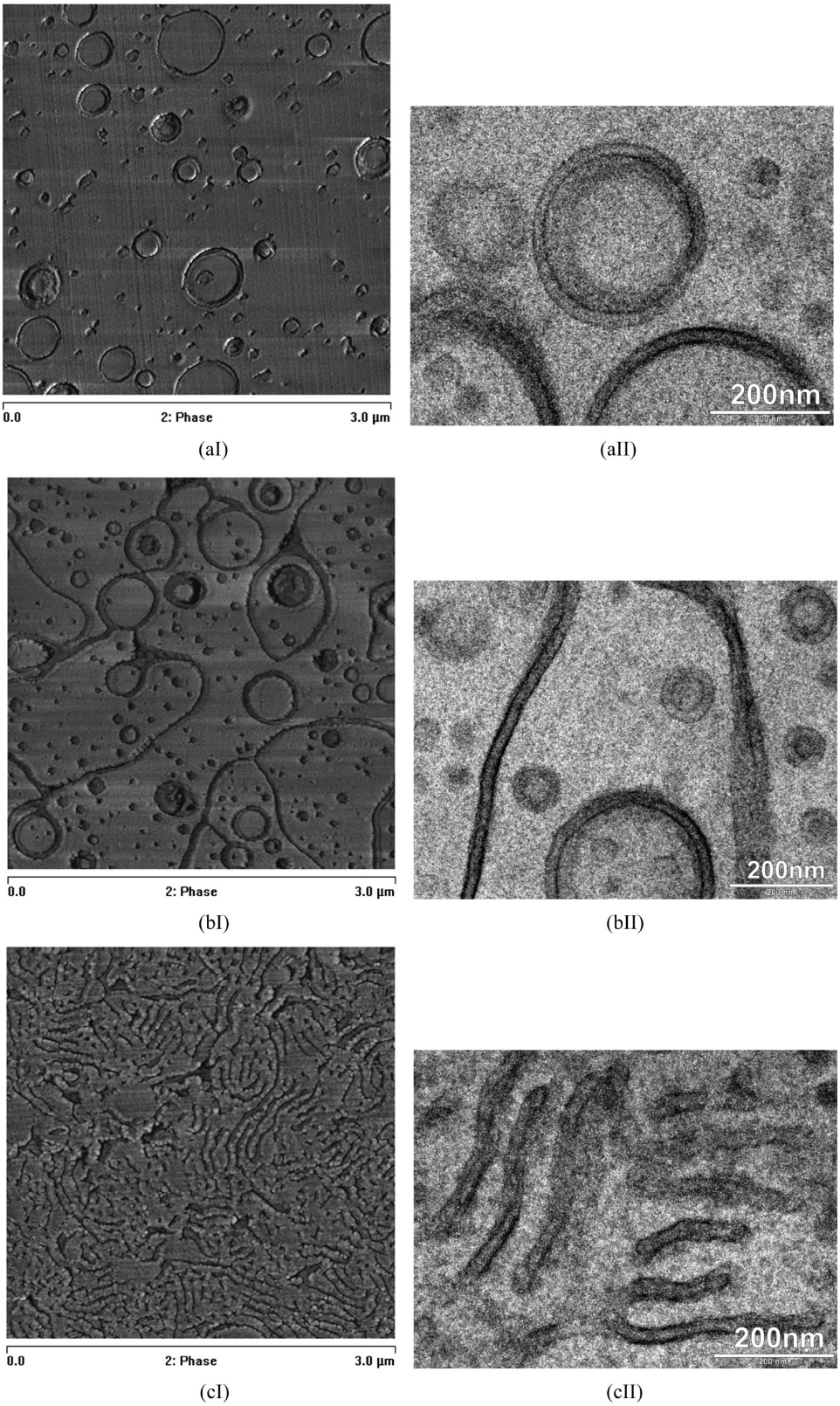

Figure 5. TM-AFM phase (I) and TEM (II) images for epoxy mixtures containing several amounts of SB50(2)ep22: (a) 10 wt %, (b) 20 wt %, and (c) 30 wt %. PS block appears dark in AFM images and black in TEM images.

AFM images (I) and TEM (II) micrographs of 10 and 30 wt % mixtures. It can be seen that long-range order microphase-separated morphologies were developed in both mixtures. The obtained morphologies in the range of composition of 10 wt % SB65ep28 were spherical micelles of segregated PS block dispersed in an epoxy matrix containing PBep block. The increase of SB65ep28 content up to 30 wt % in the mixture led to more closely packed PS micelles finely dispersed in the epoxy matrix. It is important to emphasize that in this case the formation of resulting morphologies

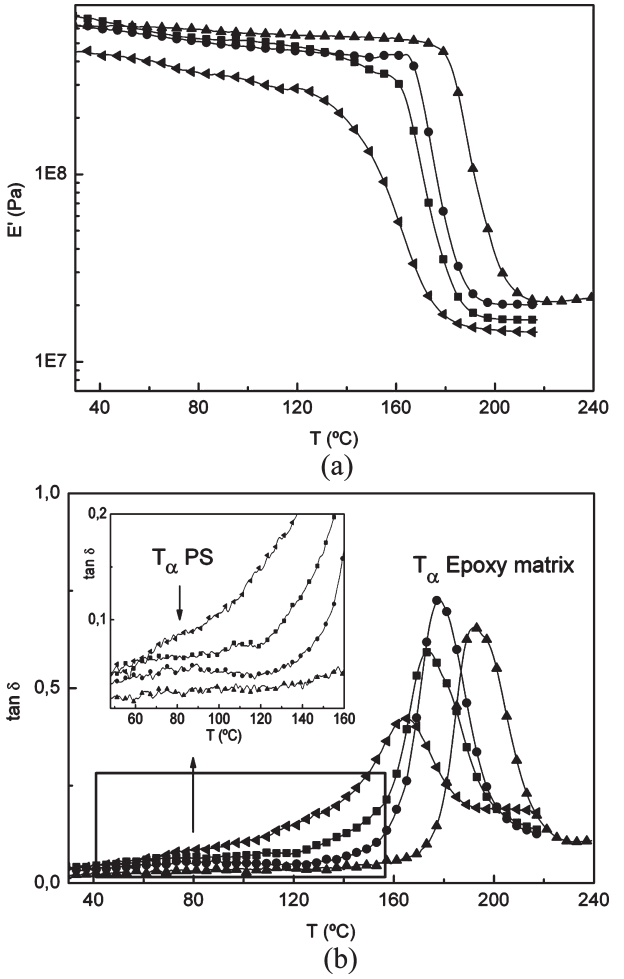

Figure 6. DMA spectra of (a) storage modulus, E', and (b) loss factor, tan δ, obtained at 1 Hz for neat epoxy (▲) and its mixtures containing SB50(2)ep22: 10 wt % (●), 20 wt %, (■) and 30 wt % (tilted ▲).

took place only by reaction-induced microphase separation of PS block starting from a totally miscible mixture before curing. In this case, the epoxidation degree was enough to make compatible the entire PBep block with the epoxy precursor. The amount of PBep was 6.5 wt % in the 30 wt % SB65ep28 mixture, thus being higher than the minimum threshold established.[20] The microphase separation of PS block was corroborated by DMA experiments (not show here); the curves revealed two T_α's, the first at around 80 °C attributed to PS phase and the second transition ascribed to T_α of epoxy matrix at 167 °C for 10 wt % SB65ep28 and 160 °C for 30 wt % SB65ep28. In addition, at temperatures higher than T_α of the epoxy-rich phase, all the systems showed a rubberlike behavior, thus confirming that this phase acted as matrix of the mixture.

Finally, schematic representations about the possible organization of blocks during the formation of nanostructures obtained in epoxy thermosets modified with SB50(2)ep22 and SB65ep28 before and after epoxy curing reaction are shown in Figure 10. Figure 10I,II shows the morphology development through PBep block self-assembly before curing followed by reaction-induced microphase separation of PS block, leading to vesicles and wormlike micelles with bilayered structure depending on the content of BC. Figure 10III shows the morphology development by reaction-induced microphase separation of PS block from a

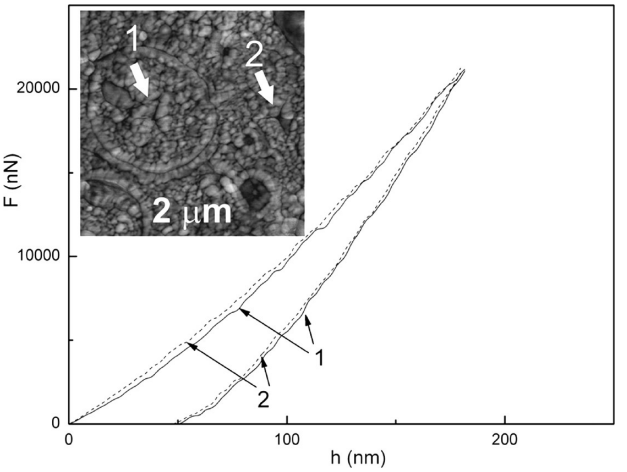

Figure 7. Force−indentation curves for 10 wt % SB50(2)ep22 mixture, inside (1, solid line) and outside of the vesicles (2, dashed line). AFM phase image is shown in the inset.

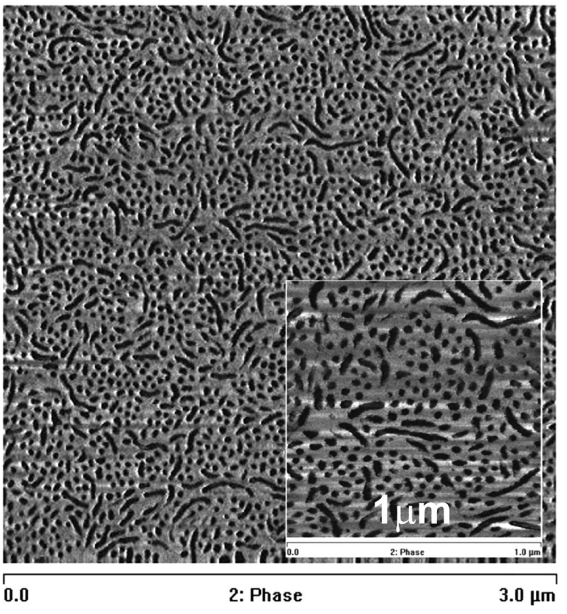

Figure 8. TM-AFM phase image for epoxy mixture containing 30 wt % SB50(1)ep35. PS block appears dark in AFM images.

totally miscible mixture before curing, leading to long-range order nanostructures after reaction. The different mechanisms involved in the morphology development mainly depend on the content of epoxidized polybutadiene in the epoxy mixture. SB65ep28 and SB50(1)ep35 show higher miscibility with epoxy resin than SB50(2)ep22 since the epoxidized PB units in the overall epoxy mixture are 6.5, 6.2, and 4 wt %, respectively, being for the systems modified with SB50(2)ep22 lower than the minimum threshold established of PBep units in the overall mixture to ensure nanostructuring. Thus, it is reasonable to expect that the mixture containing a minor number of epoxidized PB units (SB50(2)ep22) forms vesicular assemblies with a less-curved interface with the epoxy resin (Figure 5) than does the mixture with a larger number of epoxidized PB units (SB65ep28), which forms spherical micelles (Figure 9).

Fracture Toughness of Thermosetting Mixtures. Table 2 summarizes the mechanical properties of the thermosetting mixtures. It is worth to note the flexural modulus decreased

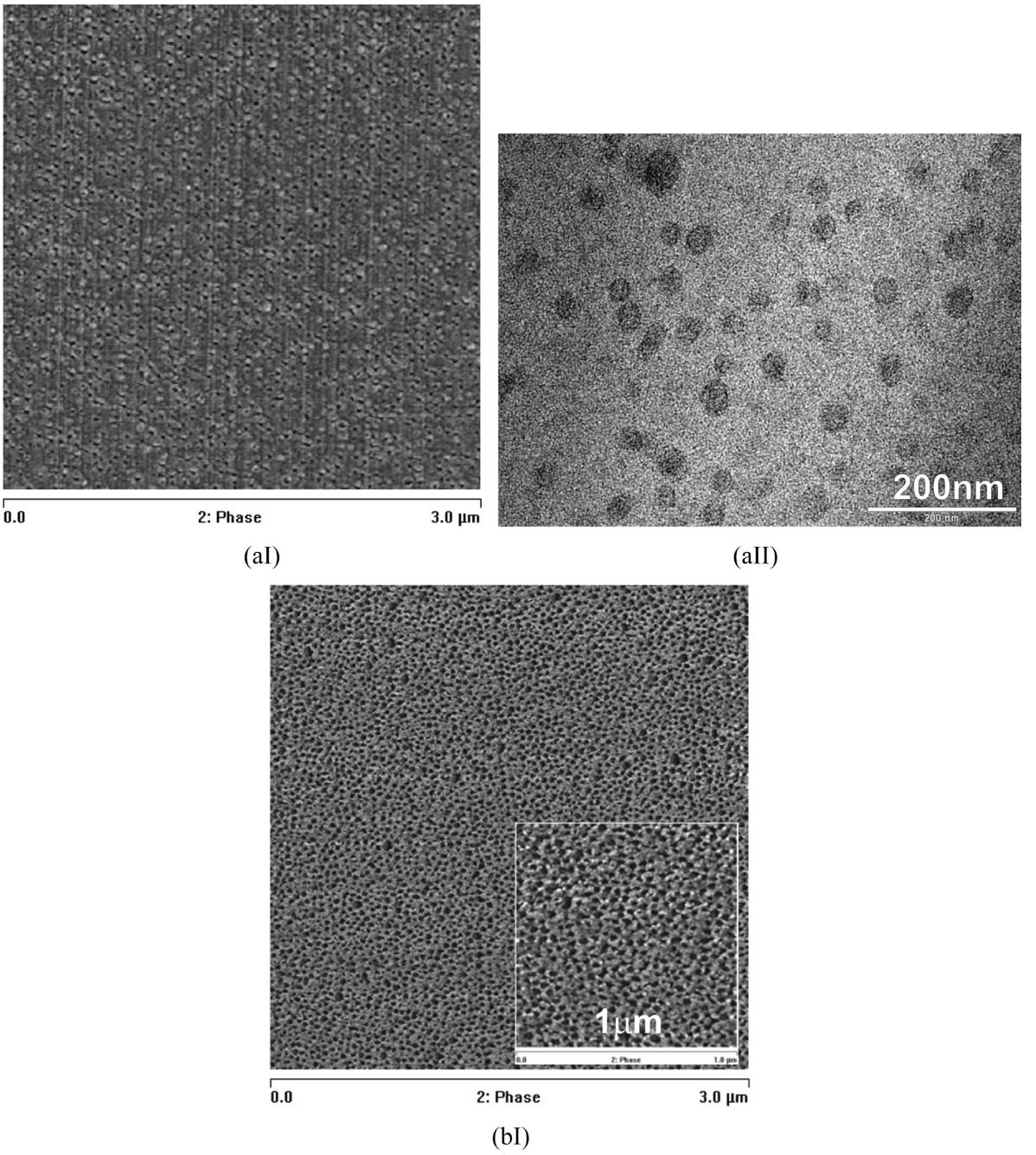

Figure 9. TM-AFM phase (I) and TEM (II) images for epoxy mixtures containing SB65ep28: (a) 10 wt % and (b) 30 wt %. Scale bar: 200 nm for TEM image. PS block appears dark in AFM images and black in TEM images.

as the content of BC in the mixture was higher. This decrease can be attributed to the plasticization effect by the incorporation of BC chains in the epoxy network. Moreover, contrary to that could be expected, modulus decrease was less for the mixtures containing SB65ep28 than for those containing SB50(2)ep22, thus demonstrating that long-range order microstructuration produced a synergistic effect on this mechanical property due to a higher extent of interactions between phases. In fact, for the same copolymer content the lower modulus appeared for the macroscopically phase-separated system being the intermediate value that for the system nanostructured without long-range order, which seems to be related to the different miscibility extents of these systems.

On the other hand, the epoxy matrix was clearly toughened for all block copolymer modified systems. As reported by other authors, G_{Ic} depends on the size and shape of the microstructure of the system.[21,22,25,28] Thus, the mixtures containing SB65ep28 that presented nanometer-sized spherical PS micelles revealed a lower contribution to fracture toughness improvement than the nanostructured mixtures containing SB50(2)ep22, these values being lower for the macroscopically phase separated mixtures with similar compositions. These results seem to indicate that the domain size of phase-separated systems is not the only factor contributing to fracture toughness enhancement but the extent of interactions at the interface between the epoxy matrix and phase-separated domains as well as their domain shape can also be relevant factors. More work with thermosetting systems showing different morphologies and several extents of miscibility between separated phases would help to know the real contribution of both factors.

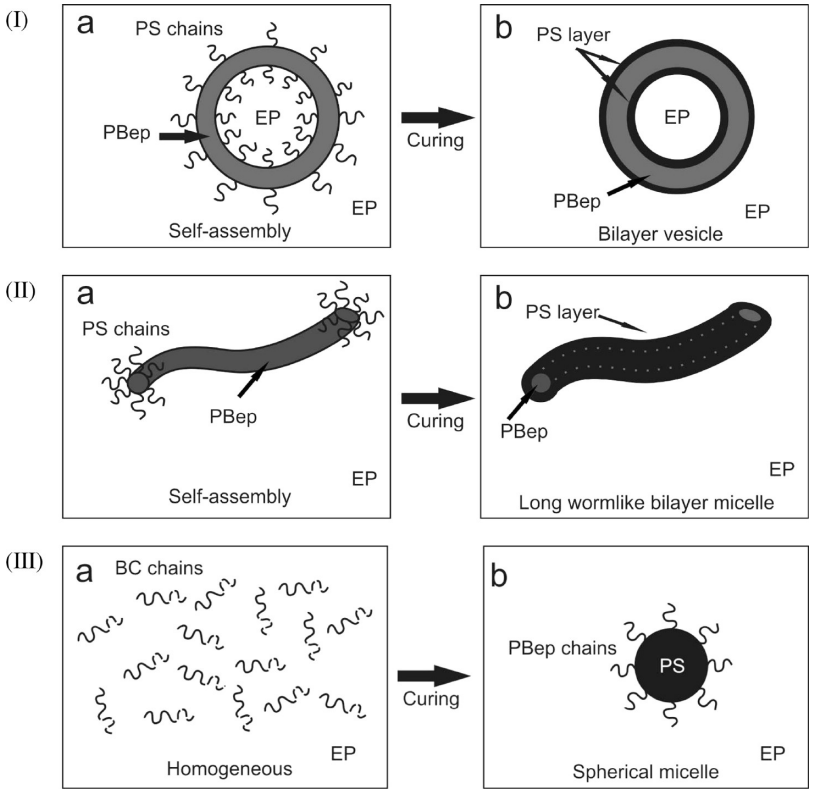

Figure 10. Schematic representations of blocks organization for the thermosetting mixtures containing: (I) 10 wt % SB50(2)ep22, (II) 30 wt % SB50(2)ep22, and (III) 10 wt % SB65ep28 block copolymers before (a) and after curing (b).

Table 2. Summary of K_{Ic} and G_{Ic} Results for Epoxy Systems Modified with Epoxidized Diblock Copolymers

system	weight (%)	E (MPa)	K_{Ic} (MPa m$^{1/2}$)	G_{Ic} (J/m^2)	$G_{Ic}/G_{Ic,epoxy}$
epoxy matrix		2700 ± 45	0.80 ± 0.02	208 ± 10	1
SB50(2)ep15	10	2200 ± 55	1.01 ± 0.09	405 ± 70	1.96
SB50(2)ep15	30	935 ± 40	0.77 ± 0.05	560 ± 75	2.69
SB50(2)ep22	10	2150 ± 80	1.00 ± 0.03	410 ± 30	1.97
SB50(2)ep22	20	1700 ± 80	0.90 ± 0.04	415 ± 40	1.99
SB50(2)ep22	30	1570 ± 60	1.31 ± 0.06	955 ± 90	4.59
SB65ep28	10	2370 ± 85	0.87 ± 0.07	285 ± 50	1.36
SB65ep28	20	2170 ± 110	0.96 ± 0.03	370 ± 20	1.78
SB65ep28	30	2060 ± 60	1.25 ± 0.07	670 ± 80	3.22

4. Conclusions

We have found with this study two main results: (1) an epoxidation degree of SB diblock copolymers, near the minimum threshold established to achieve nanostructuration in this type of thermosetting mixtures,[20] can produce microphase separation through self-assembly of epoxidized polybutadiene block and reaction-induced microphase separation of PS block, and (2) new bilayered structures are developed by the occurrence of these two mechanisms of morphology formation before and during curing reaction, leading to vesicles or long wormlike micelles depending on the concentration of block copolymer in the overall mixture. On the other hand, when the epoxidation degree is considerable lower than the minimum threshold, macrophase separation occurred as expected. Nevertheless, at higher epoxidation degree, long-range order microstructures of PS were obtained as a consequence of reaction induced microphase separation because the initial miscibility of both blocks with the epoxy resin before curing.

For fracture toughness of this kind of thermosetting mixtures, it seems that the domain size of phase-separated systems is not the only factor contributing to toughness enhancement but the extent of interactions between the phase separated domains and their domain shape can also be relevant factors. More work with thermosetting systems showing different morphologies and several extents of miscibility between separated phases would help to know the real contribution of both factors.

Acknowledgment. This work was carried out with the support of Basque Country Governments in the frame of Grupos Consolidados (IT-365-07), inanoGUNE (IE08-225), and SAIOTEK (S-PE07UN39) projects and also the Spanish Ministry of Science and Innovation for MAT2006-06331 (FUNAN). The authors thank Sergio Corona-Galván (Repsol-YPF) for the synthesis of SB block copolymers.

References and Notes

(1) Hillmyer, M. A.; Lipic, P. M.; Hadjuk, D. A.; Almdal, K.; Bates, F. S. *J. Am. Chem. Soc.* **1997**, *119*, 2749–2750.
(2) Lipic, P. M.; Bates, F. S.; Hillmyer, M. A. *J. Am. Chem. Soc.* **1998**, *120*, 8963–8970.
(3) Ritzenthaler, S.; Court, F.; David, L.; Girard-Reydet, E.; Leibler, L.; Pascault, J. P. *Macromolecules* **2002**, *35*, 6245–6254.
(4) Rebizant, V.; Abetz, V.; Tournilhac, F.; Court, F.; Leibler, L. *Macromolecules* **2003**, *36*, 9889–9896.
(5) Hermel-Davidock, T. J.; Tang, H. S.; Murray, D. J.; Hahn, S. F. *J. Polym. Sci., Part B: Polym. Phys.* **2007**, *45*, 3338–3348.
(6) Yi, F.; Zheng, S.; Liu, T. *J. Phys. Chem. B* **2009**, *113*, 1857–1868.

(7) Mijovic, J.; Shen, M.; Sy, J. W.; Mondragon, I. *Macromolecules* **2000**, *33*, 5235–5244.
(8) Grubbs, R. B.; Dean, J. M.; Broz, M. E.; Bates, F. S. *Macromolecules* **2000**, *33*, 9522–9534.
(9) Larrañaga, M.; Gabilondo, N.; Kortaberria, G.; Serrano, E.; Remiro, P.; Riccardi, C. C.; Mondragon, I. *Polymer* **2005**, *46*, 7082–7093.
(10) Larrañaga, M.; Arruti, P.; Serrano, E.; de la Caba, K.; Remiro, P.; Riccardi, C. C.; Mondragon, I. *Colloid Polym. Sci.* **2006**, *248*, 1419–1430.
(11) Meng, F.; Zheng, S.; Zhang, W.; Li, H.; Liang, Q. *Macromolecules* **2006**, *39*, 711–719.
(12) Ocando, C.; Serrano, E.; Tercjak, A.; Peña, C.; Kortaberria, G.; Calberg, C.; Grignard, B.; Jerome, R.; Carrasco, P. M.; Mecerreyes, D.; Mondragon, I. *Macromolecules* **2007**, *40*, 4068–4074.
(13) Meng, F.; Xu, Z.; Zheng, S. *Macromolecules* **2008**, *41*, 1411–1420.
(14) Fan, W.; Wang, L.; Zheng, S. *Macromolecules* **2009**, *42*, 327–336.
(15) Jian, X.; Hay, A. S. *J. Polym. Sci., Part A: Polym. Chem.* **1991**, *29*, 1183–1189.
(16) Serrano, E.; Larrañaga, M.; Remiro, P. M.; Mondragon, I.; Carrasco, P. M.; Pomposo, J. A.; Mecerreyes, D. *Macromol. Chem. Phys.* **2004**, *205*, 987–996.
(17) Serrano, E.; Martin, M. D.; Tercjak, A.; Pomposo, J. A.; Mecerreyes, D.; Mondragon, I. *Macromol. Rapid Commun.* **2005**, *26*, 982–985.
(18) Serrano, E.; Tercjak, A.; Kortaberria, G.; Pomposo, J. A.; Mecerreyes, D.; Zafeiropoulos, N. E.; Stamm, M.; Mondragon, I. *Macromolecules* **2006**, *39*, 2254–2261.
(19) Serrano, E.; Tercjak, A.; Ocando, C.; Larrañaga, M.; Parellada, M. D.; Corona-Galván, S.; Mecerreyes, D.; Zafeiropoulos, N. E.; Stamm, M.; Mondragon, I. *Macromol. Chem. Phys.* **2007**, *208*, 2281–2292.
(20) Ocando, C.; Tercjak, A.; Serrano, E.; Ramos, J. A.; Corona-Galván, S.; Parellada, M. D.; Fernández-Berridi, M. J.; Mondragon, I. *Polym. Int.* **2008**, *57*, 1333–1342.
(21) Dean, J. M.; Lipic, P. M.; Grubbs, R. B.; Cook, R. F.; Bates, F. S. *J. Polym. Sci., Part B: Polym. Phys.* **2001**, *39*, 2996–3010.
(22) Thio, Y. S.; Wu, J.; Bates, F. S. J P. *J. Polym. Sci., Part B: Polym. Phys.* **2009**, *47*, 1125–1129.
(23) Ritzenthaler, S.; Court, F.; David, L.; Girard-Reydet, E.; Leibler, L.; Pascault, J. P. *Macromolecules* **2003**, *36*, 118–126.
(24) Dean, J. M.; Verghese, N. E.; Pham, H. Q.; Bates, F. S. *Macromolecules* **2003**, *36*, 9267–9270.
(25) Dean, J. M.; Grubbs, R. B.; Saad, W.; Cook, R. F.; Bates, F. S. *J. Polym. Sci., Part B: Polym. Phys.* **2003**, *41*, 2444–2456.
(26) Rebizant, V.; Venet, A. S.; Tournilhac, F.; Girard-Reydet, E.; Navarro, C.; Pascault, J. P.; Leibler, L. *Macromolecules* **2004**, *37*, 8017–8027.
(27) Wu, J.; Thio, Y. S.; Bates, F. S. *J. Polym. Sci., Part B: Polym. Phys.* **2005**, *43*, 1950–1965.
(28) Thio, Y. S.; Wu, J.; Bates, F. S. *Macromolecules* **2006**, *39*, 7187–7189.
(29) Larrañaga, M.; Serrano, E.; Martin, M. D.; Tercjak, A.; Kortaberria, G.; de la Caba, K.; Riccardi, C. C.; Mondragon, I. *Polym. Int.* **2007**, *56*, 1392–1403.
(30) Grubbs, R. B.; Dean, J. M.; Broz, M. E.; Bates, F. S. *Macromolecules* **2000**, *33*, 9522–9534.
(31) Liu, J. D.; Sue, H. J.; Thompson, Z. J.; Bates, F. S.; Dettloff, M.; Jacob, G.; Verghese, N.; Pham, H. *Macromolecules* **2008**, *41*, 7616–7624.
(32) Liu, J. D.; Sue, H. J.; Thompson, Z. J.; Bates, F. S.; Dettloff, M.; Jacob, G.; Verghese, N.; Pham, H. *PMSE Prepr.* **2008**, *99*, 667–670.
(33) Thompson, Z. J.; Hillmyer, M. A.; Liu, J. D.; Sue, H. J.; Dettloff, M.; Bates, F. S. *Macromolecules* **2009**, *42*, 2333–2335.
(34) Oliver, W. C.; Pharr, G. M. *J. Mater. Res.* **1992**, *7*, 1564–1583.
(35) Williams, J. G.; Cawood, M. J. *Polym. Test.* **1990**, *9*, 15–26.
(36) Hoppe, C. E.; Galante, M. J.; Oyanguren, P. A.; Williams, R. J. J.; Girard-Reydet, E.; Pascault, J. P. *Polym. Eng. Sci.* **2000**, *42*, 2361–2368.
(37) Gao, W. P.; Bai, Y.; Chen, E. Q.; Li, Z. C.; Han, B. Y.; Yang, W. T.; Zhou, Q. F. *Macromolecules* **2006**, *39*, 4894–4898.
(38) Yu, H.; Zhu, J.; Jiang, W. *J. Polym. Sci., Part B: Polym. Phys.* **2008**, *46*, 1536–1545.
(39) Petrov, P. D.; Drechsler, M.; Muller, A. H. E. *J. Phys. Chem. B* **2009**, *113*, 4218–4225.
(40) Choucair, A.; Eisenberg, A. *Eur. Phys. J. E* **2003**, *10*, 37–44.
(41) Zhang, L.; Eisenberg, A. *Science* **1995**, *268*, 1728–1731.
(42) Zhang, L.; Eisenberg, A. *Macromolecules* **1996**, *29*, 8805–8815.